Dissolved organic carbon–mediated controls dominate soil carbon mineralization in response to freeze–thaw cycles

Jiaxin Yan[1], Jinyang Zheng[1], Shuai Zhang[1], Mingming Wang[1], Ting Sun[1], Jiajun Mao[1], Zhongkui Luo[1,*]

[1]State Key Laboratory of Soil Pollution Control and Safety, Zhejiang Key Laboratory of Agricultural Remote Sensing and Information Technology, Ministry of Education Key Laboratory of Environment Remediation and Ecological Health, Zhejiang University, Hangzhou, 310012, China.*Correspondence to*: Zhongkui Luo (luozk@zju.edu.cn)

Abstract. Soil freeze–thaw cycles (FTCs) exert substantial effects on the mineralization of soil organic carbon (SOC), particularly in high–altitude and –latitude cold regions. Ongoing climate change is altering FTC frequency and duration, yet the responses of SOC mineralization to such changes remain poorly understood, limiting our ability to predict carbon cycle–climate feedbacks. Here, we incubated soils from two depths across three sites to quantify how FTC regimes regulate SOC mineralization and explore underlying controls. Across all treatments, we observed a pronounced thaw–induced pulse of CO_2 release, but more frequent freeze–thaw cycles led to more cumulative CO_2 release, given the same length of cumulative thaw days. Across treatments, mineralization was most strongly correlated to dissolved organic carbon (DOC), while being suppressed by mineralogical (free and amorphous Fe/Al oxides) and physical (aggregate–protected carbon) constraints. Partial correlations and path analyses revealed that DOC was the single most consistent predictor of mineralization, retaining its influence even when enzymatic, substrate quality, or mineralogical variables were controlled. Subsoil SOC mineralization was additionally shaped by molecular carbon composition and mineral protection. These findings reveal a vertical shift from DOC–mediated substrate accessibility to molecularly and physically constrained decomposition. Accounting for these depth–specific mechanisms will improve prediction of SOC–climate feedbacks under FTC shifts due to climate change.

1 Introduction

Soil freeze–thaw cycles (FTCs) are critical drivers of biogeochemical processes in seasonally and perennially frozen ecosystems, particularly across high–altitude and high–latitude regions (Koven et al., 2020; Schuur et al., 2015). In the Northern Hemisphere, over 55% of the land area is subjected to seasonal FTCs (Lyon et al., 2022; Obu et al., 2019; Xiang et al., 2023). These cycles, caused by oscillations of soil temperature around 0 °C, induce periodic freezing and thawing, which in turn alters soil structure, nutrient mobility, microbial activity, and substrate accessibility. As such, FTCs exert strong control over the rate and pathways of soil organic carbon (SOC) mineralization, with implications for both regional carbon budgets and global carbon–climate feedbacks (Tian et al., 2015). Climate change is rapidly modifying the FTC regimes by altering their frequency, intensity, and duration due to accelerated warming in cold regions (Sorensen et al., 2018; Zhu et al., 2019). Changes in FTC characteristics have been proposed influencing microbial activity and therefore SOC mineralization , although the direction and magnitude of these effects may vary with environmental conditions. (Yang et al., 2024). Understanding how

shifts in FTC characteristics influence SOC mineralization is essential for improving projections of soil carbon turnover under future climate conditions.

Freeze–thaw cycles can alter SOC mineralization through a suite of tightly coupled biophysical processes. Physically, freezing leads to the formation of ice crystals that disrupt soil aggregates, increasing the exposure of formerly protected organic matter when thawing (Gao et al., 2015; Vaz et al., 1992). Thawing mobilizes soluble organic compounds and nutrients, temporarily increasing the availability of substrates for microbial respiration. Biologically, repeated FTC events can cause microbial cell lysis during freeze events, releasing intracellular carbon and nutrients that fuel post–thaw microbial activity (Song et al., 2017). Extracellular enzyme profiles would be particularly important as they play a central role in catalysing carbon substrates, especially, complex organic polymers, and are sensitive to FTCs (Feng et al., 2007). Although short–term freezing may have limited negative effects on microbial activity and community composition, and microbes can recover rapidly, long–term freezing may induce microbial dormancy or even death, inactivate extracellular enzymes, and ultimately suppress microbial activity and functioning, thereby altering microbial substrate strategies such as carbon use efficiency (Foster et al., 2016; Lí et al., 2024; Miura et al., 2019). To explicitly quantify SOC dynamics as impacted by FTCs, overall, it is important to elucidate the biophysical effects of FTCs on SOC mineralization which usually varies with soil physicochemical conditions (Kim et al., 2023; Liu et al., 2022; Song et al., 2017).

Despite increasing recognition of the importance of FTCs (Meisner et al., 2021; Sullivan et al., 2012), several critical knowledge gaps remain. Most existing studies have examined FTC effects in laboratory controlled conditions using simplified freeze–thaw treatments often with fixed durations, limited cycles, and surface soils without capturing the full spectrum of FTC conditions experienced in natural settings (Campbell et al., 2014). The duration of freezing and thawing within each cycle may strongly influence microbial responses, substrate availability, and the balance between cell damage and recovery, yet remains poorly characterized. Furthermore, subsoil layers (represented here by the 70–80 cm layer, compared to the 0–10 cm topsoil) store the majority of SOC (Jobbágy and Jackson, 2000; Li et al., 2020) and may experience distinct thermal and hydrological regimes during freeze–thaw cycles, yet are rarely included in FTC studies. Lastly, ecosystem–specific differences in soil texture, organic matter quality, and microbial communities could lead to divergent FTC responses, but comparative assessments across ecosystems are limited. These gaps hinder the ability of Earth system models to capture FTC–driven carbon dynamics with sufficient mechanistic details.

In this study, we conducted a laboratory incubation experiment to investigate how SOC mineralization responds to altered FTC patterns across soils from multiple ecosystems and depths. Specifically, we tested four FTC regimes that varied in the duration of freeze and thaw phases in each cycle. This design allowed us to isolate the effects of FTC duration on microbial activity and SOC decomposition while accounting for spatial heterogeneity in soil properties. By quantifying SOC

mineralization rates, cumulative CO_2 emissions, microbial enzyme activity, microbial carbon use efficiency (CUE), dissolved organic carbon (DOC), and a series of other soil physicochemical properties, the objectives were to (1) determine how changes in freeze and thaw duration affect SOC mineralization; (2) identify controls over the response of SOC mineralization to FTC; and (3) evaluate whether these responses and controls differ across soil depths. Among these measurements, DOC was specifically included because, as a dissolved and potentially highly bioavailable carbon pool, it can respond sensitively to freeze-thaw-induced changes in substrate release and microbial transformation. In this context, DOC was used as an operational indicator of short-term changes in relatively active carbon (Yano et al., 2000; Marschner and Kalbitz, 2003). By integrating measurements across physical, chemical, and biological domains, this study aims to advance mechanistic understanding of how evolving FTC patterns reshape soil carbon cycling and to improve model representation of carbon–climate feedbacks in FTC–affected regions.

2 Materials and Methods

2.1 Study sites and soil sampling

Soil samples were collected from three sites along an elevational gradient (2400 m, 3400 m, and 4600 m) in southeastern Tibet, China (29°16′–30°3′N, 94°44′–96°56′E). The mean annual temperature (MAT) at the three sites was 11.1, 3.4 and −1.3 ℃, respectively, and the mean annual precipitation (MAP) was 844, 985 and 1057 mm, respectively. These sites differ in freeze–thaw regimes in terms of duration, intensity, and frequency, allowing assessment of the generality of freeze–thaw effects across contrasting baseline conditions. Detailed information on vegetation type and soil properties of the three sites is shown in Table S1.

In July 2023, at each elevation, three replicated plots (10 × 10 m), spaced ~100 m apart, were selected for soil sampling. Within each plot, five points were randomly selected, and soil cores were extracted using a soil corer (3.7 cm diameter). Soil samples at two depth intervals (0–10 cm and 70–80 cm) were collected. The five samples from the same depth interval were thoroughly mixed to form a composite sample. The three composite samples from the three plots were treated as three replicates for each site (n = 3). All samples placed in airtight bags, stored in a container with ice, and transferred to the laboratory. In the laboratory, composite samples were divided into two portions: (1) fresh samples, which were stored at 4 ℃ for incubation experiments and microbial properties; and (2) air–dried samples, which were air–dried at room temperature, and then sieved through a 2 mm mesh to remove gravel and roots for the analysis of soil organic carbon and other soil physicochemical properties (Table S2).

2.2 Measurements of soil organic carbon and physicochemical properties

A set of soil physicochemical properties, including soil organic carbon (SOC) with its chemical structure, total nitrogen (TN), soil pH, soil texture, gravimetric water content, concentrations of iron and aluminum oxides and among others, were measured using air–dried samples. Specifically, soil water content was determined by oven–drying fresh subsamples at 105 °C to constant weight. SOC and TN were measured using an elemental analyzer (Vario EL Cube, Elementar, Germany) after removing carbonates using dilute HCl. Soil pH was measured in a 1:2.5 (w:v) soil–water suspension using a pH electrode (Mettler Toledo, Switzerland). For soil texture, carbonates and organic matter were first removed using dilute HCl and H_2O_2, respectively, and then the dispersed samples were analyzed with a laser diffraction particle size analyzer (LS–CWM, OMEC, China) to determine sand, silt and clay content. Free oxides (i.e., Fef, Alf) and amorphous oxides (Fea, Ala) of Fe and Al were extracted using dithionite–citrate–bicarbonate (DCB) and ammonium oxalate solutions, respectively, and their concentrations were measured by inductively coupled plasma optical emission spectrometry (ICP–OES; Optima 2000, PerkinElmer, USA). Particulate organic carbon (POC) and mineral–associated organic carbon (MAOC) were determined following the method of Six et al. (1998). Briefly, soil was dispersed with sodium hexametaphosphate and passed through a 0.053 mm sieve. Materials retained on the sieve were analyzed as POC, while the filtrate was used to quantify MAOC.

The chemical structure of SOC was analyzed using solid–state ^{13}C cross–polarization magic–angle spinning nuclear magnetic resonance (^{13}C CPMAS NMR; Bruker Avance 300, Germany), following the procedure of Schmidt et al. (1997) and Mathers et al. (2002). Samples were first treated with 10% HF to remove paramagnetic materials, rinsed thoroughly, and sieved to <0.15 mm. NMR chemical shift regions were assigned as follows: 0–45 ppm (alkyl C), 45–110 ppm (O–alkyl C), 110–160 ppm (aromatic C), and 160–220 ppm (carboxyl C). The aromatic region was further divided into aryl C (110–145 ppm) and phenolic C (145–160 ppm). Ratios of alkyl C/O–alkyl C and hydrophobic C (alkyl + aromatic) to hydrophilic C (O–alkyl + carboxyl) were further calculated to characterize SOC chemical characteristics, specifically the relative abundance of alkyl versus O-alkyl C and the balance between hydrophobic and hydrophilic components (Mathers et al., 2007; Spaccini et al., 2002).

2.3 Incubation experiments and mineralization measurements

A 48–day laboratory incubation experiment was conducted to investigate the effect of freeze–thaw regimes on SOC mineralization by controlling the duration of freeze and thaw periods (Fig. S1): (1) LFLT – long freeze, long thaw: 12 days freeze followed by 12 days thaw (2 cycles in 48 days); (2) LFST – long freeze, short thaw: 12 days freeze followed by 4 days thaw (3 cycles); (3) SFLT – short freeze, long thaw: 4 days freeze followed by 12 days thaw (3 cycles); (4) SFST – short freeze, short thaw: 4 days freeze followed by 4 days thaw (6 cycles).

For the incubation, 20 g of fresh soil was placed into 150 mL polyethylene jars (total = 72; four freeze–thaw regime treatments × three sites × two soil depths × three replicates). All jars were pre–incubated at 10 ℃ for 10 days to stabilize microbial activity. Then, they were moved to incubator for incubation at –10 ℃ (freeze) and 10 ℃ (thaw) in sequence as the four freeze–thaw treatments described, with temperature fluctuations controlled within ± 0.5 ℃. Additionally, jars (500 ml, a total of three soil sites × two soil depths × four freeze–thaw treatments = 24), each containing 300 g of the fresh composite soil sample, were incubated at the same freeze–thaw regimes for monitoring microbial properties, enzyme activities, and soil carbon properties at selected time points of soil mineralization measurements (section 2.4). For all jars, soil moisture was adjusted to 60% of the saturated water-holding capacity of fresh sieved soil, as determined by the funnel method (Fierer et al., 2006), and was maintained by regular weighing and, when necessary, addition of distilled water. Saturated water-holding capacity was calculated from the difference between the volume of water added and the volume drained, plus the water originally present in the soil. The amount of water required to reach the target moisture level was then calculated based on this value and the gravimetric water content of fresh subsamples dried at 105 ℃. During incubation, jars were sealed with gas-permeable but water-impermeable membranes to prevent anaerobic conditions and limit moisture loss.

Throughout the 48–day incubation period, SOC mineralization rate was measured during both the freeze and thaw phases at days 0.25 (i.e., 6 hours after the temperature treatment), 1, 2, 4, 7, and 12, when applicable. At each of the measurement time point, the 150 mL incubation jars were placed into an automatic soil respiration measurement system (PRI–8800, Pri–Eco, Beijing, China) (Liu et al., 2017; Nianpeng et al., 2013). Each measurement lasted 3 minutes at the current incubation temperature, and SOC mineralization rates were calculated as the slope of CO_2 concentration changes over time. These measurements were linearly interpolated to estimate cumulative mineralization for the whole 48–day incubation, and for each phase (freeze and thaw). The complete Rs time-series dataset comprised 2,376 observations from the 72 respiration jars.

2.4 Measurements of dissolved organic carbon and microbial properties

At time points aligned with SOC mineralization measurements, we quantified dissolved organic carbon (DOC), extracellular enzyme activities, microbial biomass carbon (MBC), and carbon use efficiency (CUE). For DOC and enzyme activities, soils were sampled on days 1, 2, 4, 7 (for long-phase treatments only), and 12 (for long-phase treatments only). MBC and CUE were measured only on day 1 of each thaw period. For the LFLT and SFLT regimes, measurements of DOC, MBC, CUE, and enzyme activities were terminated after the first freeze–thaw cycle, whereas for the LFST and SFST regimes they were terminated after the third freeze–thaw cycle. This design ensured that all treatments were compared at the same cumulative thaw duration (12 days), thereby isolating the effect of freeze–thaw frequency on soil organic carbon mineralization while controlling for total thaw exposure. Accordingly, the thaw-phase covariate dataset comprised 504 observations in total, whereas the subset for thaw day 1, for which MBC and CUE were available, comprised 144 observations. Here, observation

refers to elevation × depth ×treatment × FT-event ×replicate combination derived from the 24 repeatedly sampled 500 mL incubation units.

To quantify DOC, 1 g of fresh soil was extracted with 0.1 M K_2SO_4 at a soil–to–solution ratio of 1:10 (w/v). The extract was centrifuged at 4000 r/min for 10 min and filtered through a 0.45 µm membrane, and DOC concentration was measured using a total organic carbon analyzer (Multi N/C 3100, Analytik Jena, Germany). MBC was determined by the chloroform fumigation–extraction method (Vance et al., 1987). Briefly, 5 g of fresh soil was fumigated with ethanol–free chloroform for 24 h, while a parallel 5 g subsample remained unfumigated. Both samples were extracted with 20 ml of 0.5 M K_2SO_4 shaken for 30 minutes, centrifuged at 4000 r/min for 10 min and filtered through 0.45 µm membranes. MBC was calculated as the difference in extractable organic carbon between the fumigated and unfumigated samples (Ec), divided by the kEC factor of 0.45, following the conventional chloroform fumigation-extraction method. The kEC value of 0.45 accounts for incomplete recovery of microbial biomass C in the extract and was originally proposed by Vance et al. (1987) and later verfied by Joergensen and Mueller (1996).

CUE was determined using the $^{18}O–H_2O$ labelling method (Schwartz, 2007; Spohn et al., 2016). One gram of soil was split into two 0.5 g subsamples, each placed in a 2 ml screw–cap vial. One vial received 60 µl of ^{18}O–labeled water (20 atom% ^{18}O), and the control received the same volume of unlabeled water. After vortexing and centrifugation, samples were incubated at 10 °C for 24 h in sealed 50 ml jars. CO_2 concentrations were measured before and after incubation to assess microbial respiration. Following incubation, soils were flash–frozen in liquid nitrogen and stored at –80 °C for DNA extraction. DNA was extracted using the MP Soil DNA Kit (FastDNATM Spin Kit for Soil, MP Biomedicals, Germany), with extended centrifugation to increase yield (Spohn et al., 2016). DNA was quantified using a NanoDrop spectrophotometer, dried in silver capsules at 60 °C for 48 h, and analyzed for ^{18}O enrichment by Isotope Ratio Mass Spectrometry (TC/EA–IRMS, Delta V Advantage, Thermo Fisher, Germany). CUE was calculated based on ^{18}O incorporation into microbial DNA relative to cumulative CO_2 production.

Potential extracellular enzyme activities (EEA) were measured using substrate-based microplate assay kits from Suzhou Grace Biotechnology Co., Ltd. (Suzhou, China), including the Solid-β-Glucosidase Kit (G0312W96), Solid-Cellobiohydrolase Kit (G0323W96), Solid-Peroxidase Kit (G0317W), and Solid-Polyphenol Oxidase Kit (G0311W). Briefly, β-1,4-glucosidase (BG, EC 3.2.1.21) activity was determined using p-nitrophenyl-β-D-glucopyranoside as the artificial substrate, and cellobiohydrolase (CBH, EC 3.2.1.91) activity was determined using p-nitrophenyl-β-D-cellobioside. In both assays, enzyme activities were quantified from the formation of p-nitrophenol (PNP) measured as the absorbance at wavelength of 405 nm. Polyphenol oxidase (PPO, EC 1.10.3.1) and peroxidase (POD, EC 1.11.1.7) activities were determined using L-3,4-dihydroxyphenylalanine (L-DOPA)-based colorimetric assays, with absorbance measured at 475 nm; POD was assayed in the

presence of H_2O_2. For all enzymes, soil samples were incubated with the corresponding assay reagents under the manufacturer-specified conditions, and enzyme activities were calculated from control-corrected absorbance values using the kit-specific equations. Enzyme activities were expressed as nmol h^{-1} g^{-1} soil. Because these assays were performed under standardized incubation conditions with artificial substrates, the reported values represent extracellular enzyme activities rather than enzyme concentrations or in situ instantaneous activities.

2.5 Statistical analyses

The Rs time-series measurements including 2,376 observations from 72 respiration jars were used to evaluate how freeze–thaw treatments, soil origin, soil depth, measurement time, and freeze–thaw cycle number influenced SOC mineralization rates. We first performed a multivariate ANOVA, followed by Tukey's HSD tests for post–hoc comparisons. Cumulative mineralization over the entire 48–day incubation, as well as cumulative mineralization during thaw and freeze phases, was compared among the four freeze–thaw treatments and between soil depths. Prior to all parametric analyses, data normality was assessed using Shapiro–Wilk tests and homogeneity of variance using Bartlett's tests; logarithmic transformation was applied when assumptions were not met.

To identify key covariates underlying mineralization responses, we initially focused on data from day 1 of the thaw period, the only time point at which MBC and CUE were measured. For analyses linking SOC mineralization rates with DOC, EEA, MBC, CUE, and other soil properties, we averaged the Rs values from three 150 mL respiration jars corresponding to each combination of elevation × soil depth × freeze–thaw treatment × sampling time × replicate, and matched them to the covariate measurements obtained from the corresponding 500 mL incubation jar. Consequently, the thaw day 1 dataset used for covariate analyses initially comprised 144 observations, and the full thaw-phase dataset used for repeated covariate analyses initially comprised 544 pooled observations. To unify the analytical unit and avoid pseudo-replication, the three biological replicates under each treatment, soil depth, elevation, and sampling time were averaged prior to subsequent statistical analyses, yielding a representative value for each time point. Thus, the dataset for thaw day 1 analyses contained 48 observations, and the dataset for the full thaw phase contained 168 observations. We used two-way ANOVA to characterize the effects of freeze-thaw treatment and soil depth on soil physicochemical and microbial variables, followed by Tukey's HSD for multiple comparisons. Within-treatment depth differences and within-depth treatment differences were summarized using significance groupings based on LSD tests with Bonferroni correction. We then fitted linear regressions of SOC mineralization rate (Rs) against each measured soil property. To examine whether the patterns observed on day 1 generalize across the thaw period, the same processes were repeated for additional time points where covariate data were available. We then performed univariate partial correlation analyses for day 1 of the thaw period, in which each variable was controlled in turn. These partial correlations quantify the unique association between Rs and a given predictor after removing variance attributable to another predictor, thereby revealing potential dependency relationships among covariates.

To distinguish differences among freeze–thaw treatments and soil depths in the relationship between dissolved organic carbon (DOC) and SOC mineralization rate (Rs), a linear mixed-effects model was fitted using all observations collected during the thawing phases across the entire incubation period. Prior to model fitting, DOC was mean-centred to improve parameter interpretability and reduce collinearity between fixed and random effects in the random-slope model. The model was specified as: Rs ~ DOC + (1 + DOC | Treatment) + (1 + DOC | Depth), where Rs is the SOC mineralization rate, DOC denotes mean-centred DOC, and Treatment and Depth represent freeze–thaw regime and soil depth, respectively. In this model, DOC was included as a fixed effect to estimate the overall DOC–Rs relationship, whereas Treatment and Depth were specified with both random intercepts and random slopes to allow group-specific variation in baseline Rs and in the strength of the DOC effect. The model therefore quantified both the overall average effect of DOC and the heterogeneity of this relationship among treatments and soil depths.

To disentangle the direct and indirect effects of freeze–thaw regimes on SOC mineralization, we applied partial least squares path modeling (PLS–PM) using all observations collected during thaw phases, with Rs as the response variable. Prior to model construction, we screened predictors using variance inflation factors (VIFs) and sequentially removed non–focal variables with VIF > 10 to reduce multicollinearity (Dormann et al., 2013). The categorical treatment factor (four freeze–thaw regimes) was retained by expanding it into dummy variables, which served as reflective indicators of a latent "Treatment" construct, enabling the PLS–PM framework to represent treatment differences as a single exogenous driver (Hair et al., 2017). In addition, incubation time was included as an exogenous variable to capture temporal dynamics across the thawing phases. Specifically, time was coded as the incubation time corresponding to each measurement point, from the beginning to the end of the experiment, and was incorporated into the model as a single-indicator latent construct (Time). This allowed temporal variation during the incubation process to be explicitly separated from treatment effects and other covariates. The final PLS–PM structure included seven latent variables (Table S2). Separate models were fitted for topsoil and subsoil. Significance of structural path coefficients was evaluated using non–parametric bootstrap resampling (95% bootstrap confidence intervals). All variables were standardized prior to analysis. PLS–PM was conducted using the plspm package in R, and all statistical analyses were completed in R version 4.0.3 (http://cran.r–project.org/).

3 Results

3.1 The effects on mineralization rates

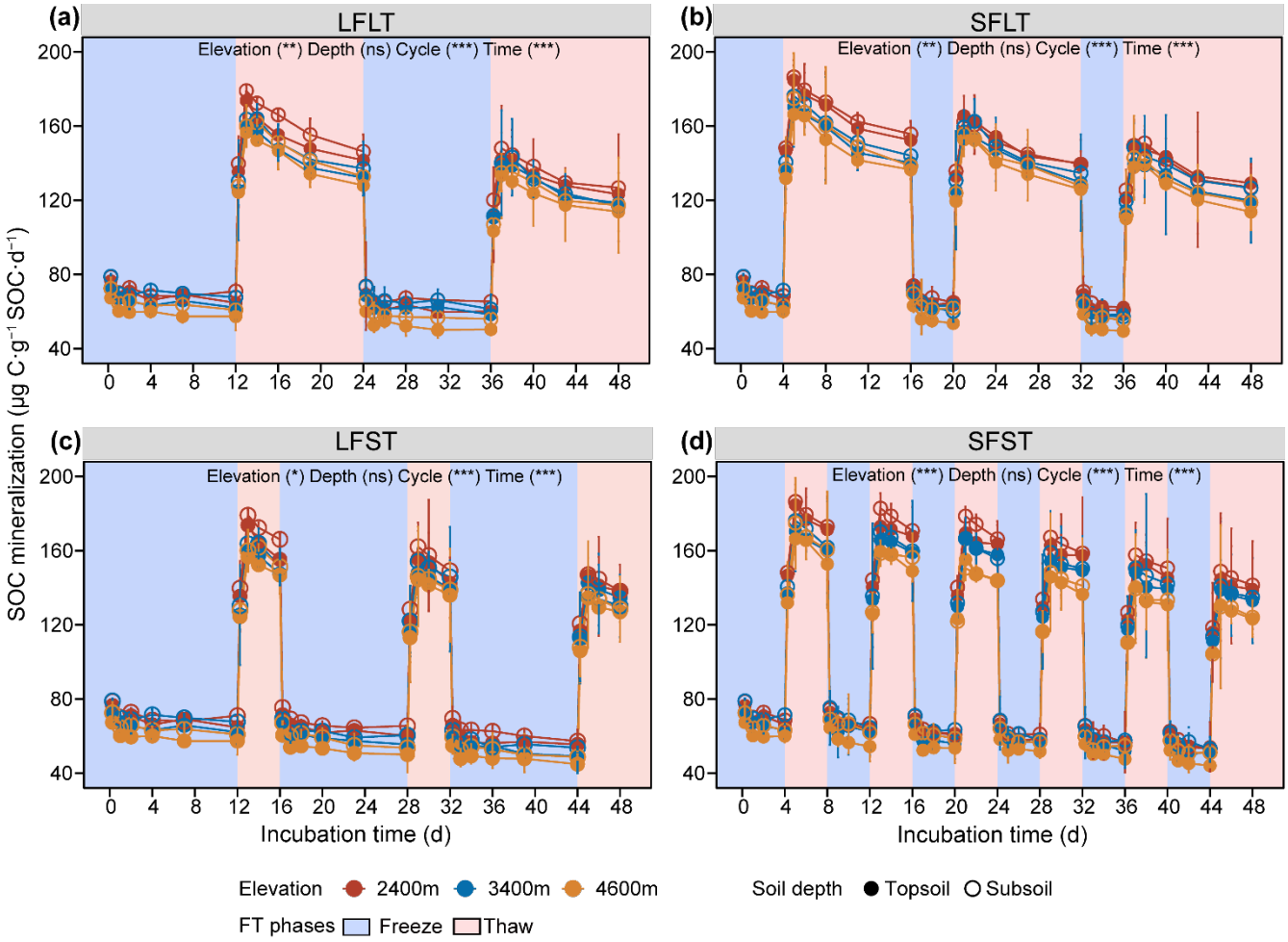

Figure 1: Soil organic carbon (SOC) mineralization rate during freeze–thaw cycle incubation. Soil was incubated for 48 days under two temperature conditions: –10°C (Freeze) and 10°C (Thaw). Four distinct freeze–thaw cycle patterns were designed to address knowledge gaps in previous studies, based on two cycle durations: 12–day (long) and 4–day (short). Panels a–d show the temporal dynamics of SOC mineralization under the four freeze–thaw regimes: (a) long freeze–long thaw (LFLT), (b) short freeze–long thaw (SFLT), (c) long freeze–short thaw (LFST), and (d) short freeze–short thaw (SFST). The blue and red background areas denote freezing (–10 °C) and thawing (10 °C) phases, respectively. Data points represent treatment means ± 1 SE (n = 3). Significance tests compare elevations, soil depths, cycle number, and incubation time during thaw periods (*, $p < 0.05$; **, $p < 0.01$; ***, $p < 0.001$).

Carbon mineralization exhibited pronounced phase–dependent dynamics across all freeze–thaw regimes, soil depths, and sites (Fig. 1). During each thaw phase, SOC mineralization increased sharply, reaching its peak within one–occasionally two–days before declining. Peak thaw–phase mineralization ranged from 177.2 to 221.7 μg $C \cdot g^{-1}$ $SOC \cdot d^{-1}$ across treatments and soil origins. In contrast, mineralization during freezing remained comparatively low and stable (11.1–98.5 μg $C \cdot g^{-1}$ $SOC \cdot d^{-1}$), representing only 17.1–42.5% of thaw–phase peak rates.

Across successive freeze–thaw cycles, mineralization during both thaw and freeze phases declined in magnitude while maintaining their characteristic temporal patterns (Fig. 1). The magnitude of decline did not differ significantly between topsoil and subsoil ($p > 0.05$). For instance, under the LFLT treatment, cumulative mineralization in the second cycle was 13.7 ± 2.8% (mean ± SE) lower than in the first cycle. Comparable reductions were observed under LFST (6.7 ± 2.2%) and SFLT (8.1 ± 2.3%). The greatest attenuation occurred under SFST, where cumulative mineralization in the final cycle declined by 20.3 ± 2.0% relative to the initial cycle.

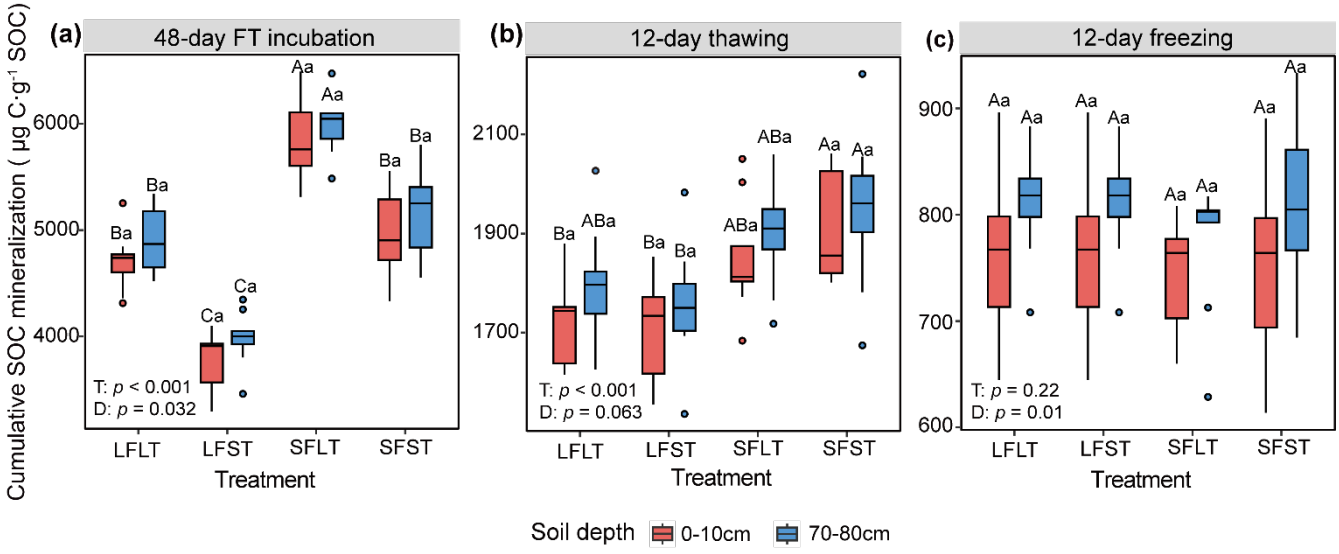

Figure 2: Cumulative soil organic carbon (SOC) mineralization under different freeze–thaw regimes and soil depths. (a) Cumulative SOC mineralization over the full 48–day freeze–thaw incubation. (b) SOC mineralization over the same 12 cumulative thaw days. (c) SOC mineralization over the same 12 cumulative freeze days. Bars represent cumulative SOC mineralization for topsoil (0–10 cm) and subsoil (70–80 cm) under each freeze–thaw treatment. Error bars indicate ±1 SE (n = 18). Uppercase letters denote significant differences among treatments within a given depth (Tukey's HSD), and lowercase letters indicate significant differences between depths within a given treatment.

Over the full 48–day incubation, cumulative mineralization differed markedly among freeze–thaw regimes. The SFLT treatment produced the highest cumulative losses, followed by SFST, LFLT, and LFST (Fig. 2a). This ordering closely reflected the total number of thaw days associated with each treatment (36, 24, 24, and 12 days, respectively). In line with this pattern, cumulative mineralization during the freeze phase did not differ among treatments when compared over the same 12 cumulative freeze days ($p = 0.22$; 767.5–851.7 μg C g^{-1} SOC; Fig. 2c). In contrast, substantial differences emerged during the thaw phase: cumulative mineralization over 12 cumulative thaw days was significantly higher under the SFST and SFLT treatments than under LFLT and LFST ($p < 0.001$; Fig. 2b). Across all freeze–thaw regimes, cumulative mineralization during both freeze and thaw phases did not differ significantly between topsoil and subsoil (Fig. 2).

3.2 The effects on DOC, microbial properties and enzyme activities

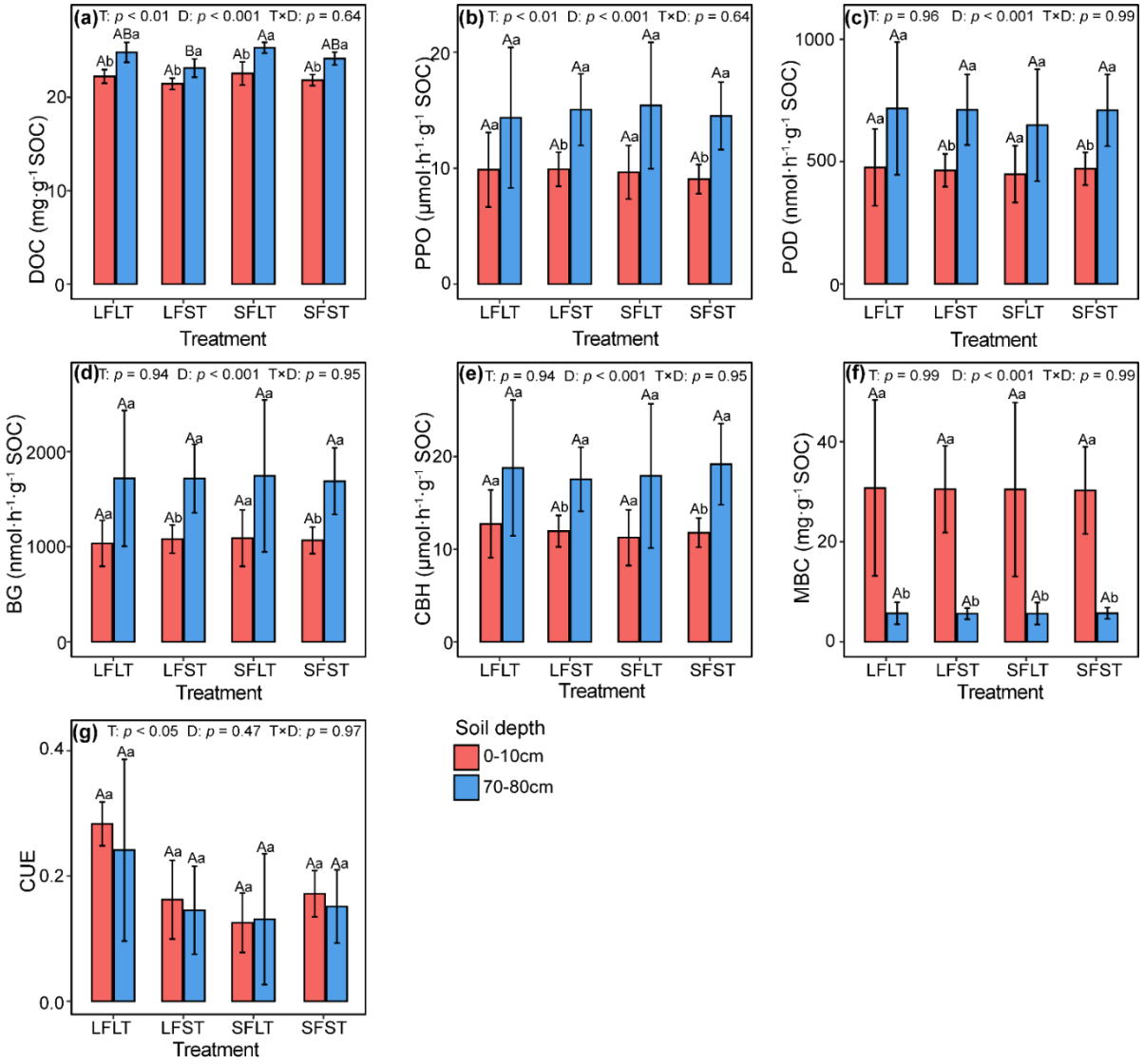

Figure 3: Effects of freeze–thaw regimes on dissolved organic, enzyme activities, and microbial properties across two soil depths. Panels (a–g) show dissolved organic carbon (DOC), polyphenol oxidase activity (PPO), peroxidase activity (POD), β–glucosidase activity (BG), cellobiohydrolase activity (CBH), microbial biomass carbon (MBC), and carbon use efficiency (CUE), respectively. Error bars indicate the variability among the repeated observations used to calculate each treatment mean, rather than independent biological replication among separate jars. Specifically, for the LFLT and SFLT treatments, *n* = 3 corresponds to measurements taken on the first day of thawing in the first freeze–thaw cycle, whereas for the LFST and SFST treatments，, *n* = 9 corresponds to measurements taken on the first day of thawing across the first to third freeze–thaw cycles. Different uppercase letters indicate significant differences among treatments within the same soil depth, whereas different lowercase letters indicate significant differences between soil depths within the same treatment (Tukey's multiple comparison test).

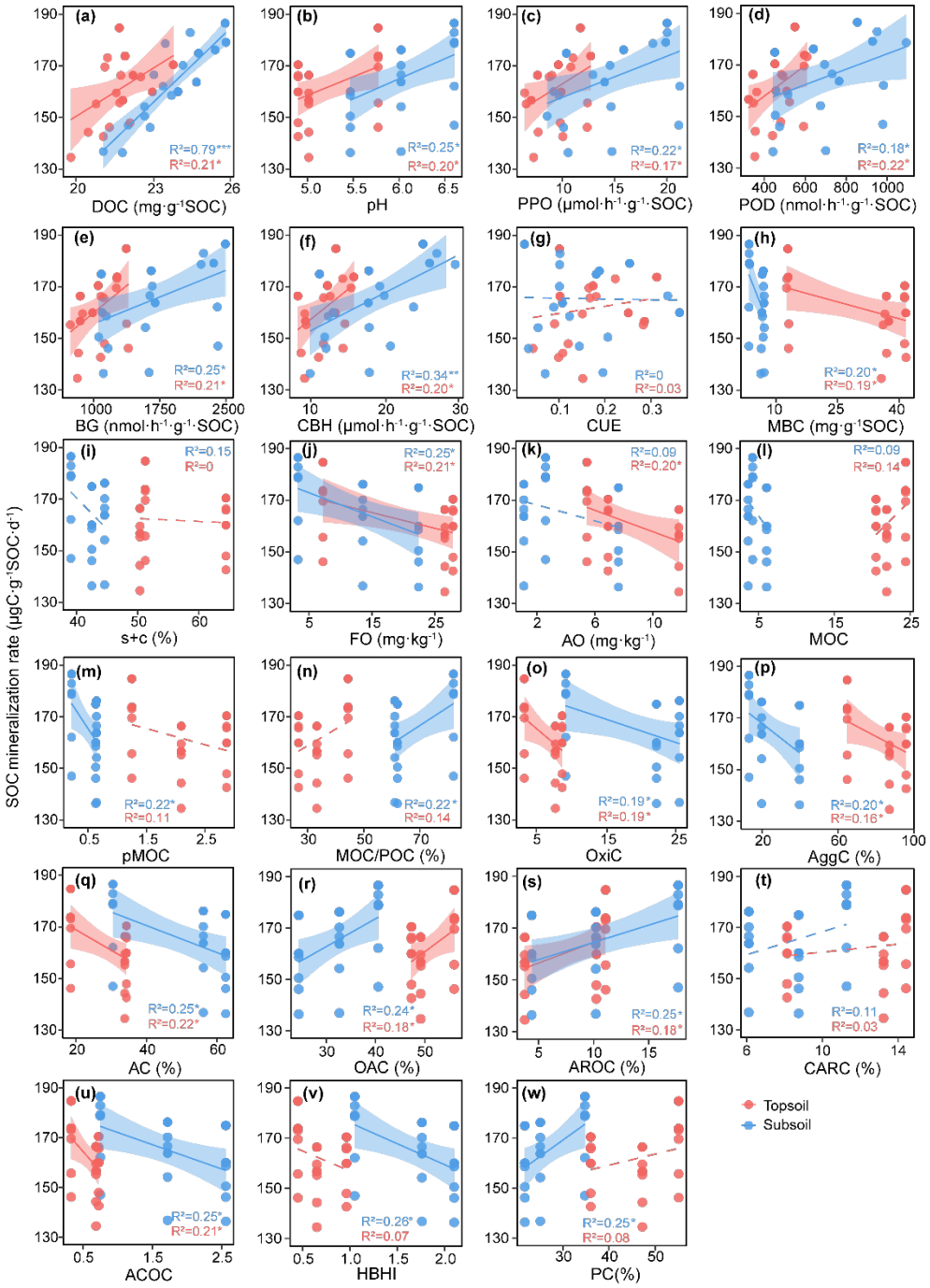

Figure 4: Relationships between soil properties and soil organic carbon (SOC) mineralization rate. Red and blue symbols represent the topsoil and subsoil, respectively. Solid lines indicate significant linear regressions, whereas dashed lines indicate non–significant relationships. Asterisks denote levels of statistical significance: *, $p < 0.05$; **, $p < 0.01$; ***, $p < 0.001$. R^2 shows the determination coefficient of the regression. For LFLT and SFLT, measurements correspond to the first thawing day of the first freeze–thaw cycle; for LFST and SFST, measurements correspond to the first thawing day of the first, second, and third freeze–thaw cycles. Abbreviations of soil properties are defined in Table S2.

Freeze–thaw regimes exerted strong but variable effects on DOC and enzyme activities–two functional groups most directly linked to SOC mineralization. DOC showed a dynamic change over time, exhibiting pulsed patterns broadly consistent with SOC mineralization rates (Fig. S3). On the first thawing day (Fig. 3; Fig. 4), when the most complete covariate dataset was available (n = 48), DOC concentrations were significantly affected by freeze-thaw treatment (ANOVA, $p < 0.01$; Fig. 3a). Post hoc comparisons further showed that, at the 70–80 cm layer, DOC concentrations were significantly higher under SFLT than under LFST, whereas the other pairwise comparisons were not significant. However, enzyme activities did not show significant differences across treatments in either the topsoil or subsoil on the first thawing day (Fig. 3b-e). Hydrolytic enzymes (BG, CBH) and oxidative enzymes (PPO, POD) were not as significantly elevated as DOC under high–frequency regimes. In contrast, enzyme activities under low–frequency regimes remained relatively low. When considered across the full thaw phase, the paired covariate dataset comprised 168 pooled observations, allowing comparison of whether the DOC and enzyme activity patterns observed on thaw day 1 were representative of later thaw stages (Fig. S3)

Microbial biomass carbon showed limited sensitivity to freeze–thaw treatments (Fig. 3f; Fig. 4h). Although some fluctuations occurred, treatment–level differences were small compared with those observed for DOC and enzymes, suggesting that freeze–thaw frequency influences microbial function and substrate supply more strongly than population size. Carbon use efficiency also remained stable across regimes (Fig. 3g), further indicating that the primary microbial responses to freeze–thaw cycling occurred through changes in substrate accessibility rather than shifts in microbial growth efficiency.

3.3 Predictors of mineralization rates

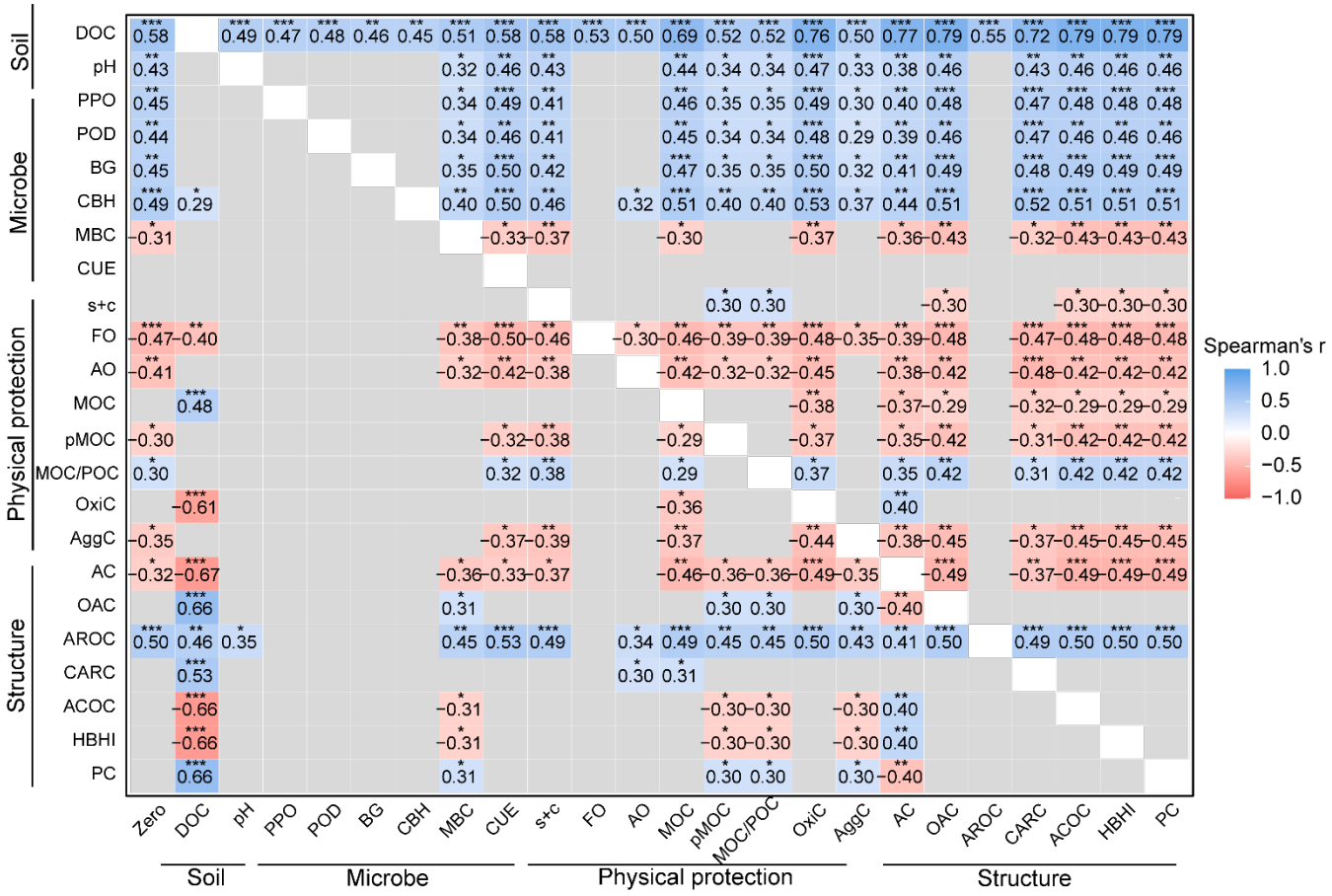

Figure 5: Partial correlations (Spearman's r) of soil organic carbon (SOC) mineralization with soil physicochemical and biological properties. The first column shows the zero-order correlations between SOC mineralization and the respective soil factors, without controlling for any other variables. Subsequent columns represent partial correlations, where the relationship between the variables is calculated after controlling for the corresponding factor along the x-axis. The colour and numbers indicate the strength and sign of the correlation. Blank cells indicate that the corresponding factor in the row is controlled and therefore no correlation is computed for that pair of variables. Gray cells represent non-significant correlations, while colored cells indicate significant correlations, with blue shades reflecting positive correlations and red shades reflecting negative correlations. The intensity of the color indicates the strength of the correlation. Statistical significance is indicated by asterisks (*, $p < 0.05$; **, $p < 0.01$; ***, $p < 0.001$). Abbreviations of the variables are explained in Table S2.

After pooling the data from the first thawing day (on this day we have the most comprehensive measurements) across all freeze–thaw treatments, mineralization rates showed strong associations with indicators of substrate availability, molecular composition, and catalytic potential (Fig. 5). Positive correlations ($p < 0.05$) were observed with DOC (Spearman's $r = 0.58$), AROC ($r = 0.50$), and hydrolytic and oxidative enzymes including CBH ($r = 0.49$), BG ($r = 0.45$), PPO ($r = 0.45$), and POD ($r = 0.44$). Mineralization also increased modestly with soil pH ($r = 0.43$) and the MOC/POC ratio ($r = 0.30$, Fig. 5). In contrast, negative associations were detected with MBC ($r = –0.31$), free Fe/Al oxides ($r = –0.47$), amorphous oxides ($r = –0.41$), alkyl

C (r = –0.32), and aggregate–protected carbon (AggC, r = –0.35), indicating stronger mineralogical and physical constraints where these fractions were more abundant.

Partial correlation analysis provided further insight into hierarchical relationships among DOC, enzymatic activity, and molecular structure (Fig. 5). After controlling for enzyme activities, all correlations except that with DOC became insignificant, suggesting that enzyme activity integrates information on microbial functioning and general substrate availability. In contrast, the correlation between mineralization and DOC remained significant regardless of which variables were controlled, highlighting its distinct and dominant role as an immediately utilizable carbon pool. Controlling for DOC generated substantial shifts in associations with molecular C fractions. For instance, the negative correlation with alkyl C strengthened from r = –0.32 to –0.67. Additional significant associations emerged with O–alkyl C (r = 0.66), carboxylic C (r = 0.53), the AC/OAC ratio (r = –0.66), the hydrophobic–hydrophilic ratio (r = –0.66), and polysaccharide C (r = 0.66), indicating that once DOC effects are accounted for, mineralization is strongly structured by the quality and functional–group distribution of remaining SOC.

Separating the dataset by depth revealed striking vertical differentiation in the controls of SOC mineralization (Fig. S7). In both layers, DOC and enzyme activities remained significant zero–order predictors (Fig. S7), confirming their importance throughout the profile. However, the nature of secondary controls diverged with depth. Topsoil mineralization was primarily associated with DOC and enzyme activity, whereas relationships with molecular C fractions were weak. By contrast, subsoil mineralization exhibited strong additional associations with C molecular composition (e.g., AC, OAC, ACOC, HBHI, PC), reflecting greater chemical and physical constraints on substrate decomposability at depth. Partial correlations reinforced this depth pattern. In the topsoil, controlling for DOC substantially altered relationships with multiple variables; the same effect appeared when controlling for soil texture (silt + clay). In the subsoil, however, controlling for pH, PPO, bulk density, CBH, free Fe/Al oxides, AggC, or molecular composition removed almost all remaining correlations, leaving DOC as the only consistent predictor (Fig. S7). This pattern indicates a transition from a biologically dominated system in the topsoil to one where substrate chemistry and mineralogical protection exert stronger control in the subsoil.

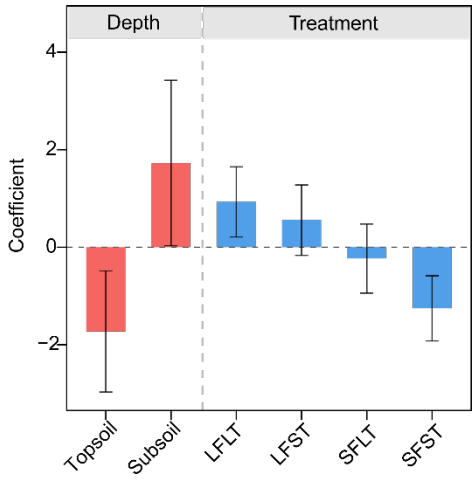

Figure 6: The effects of DOC on Rs. Bars show the random-slope deviations of the DOC effect on Rs relative to the overall fixed slope, based on the linear mixed-effects model Rs~DOC+(1+DOC|Treatment)+(1+DOC|depth) , where DOC denotes mean-centred DOC. The model was fitted using all observations collected during the thawing phases throughout the entire freeze–thaw incubation period (n = 168). Positive values indicate a stronger DOC–Rs relationship than the overall average, whereas negative values indicate a weaker relationship. Error bars represent 95% confidence interval.

Using data from all thawing phases across the entire incubation period (n = 168), the linear mixed-effects model showed a significant positive effect of DOC on Rs, with a fixed slope of 6.7 ± 1.9 (t = 3.5; Table S5). The marginal and conditional coefficients of determination were $R^2m = 0.56$ and $R^2c = 0.72$, respectively, indicating that the fixed effects alone explained 56% of the variation in Rs, whereas inclusion of group-level variation associated with Treatment and Depth increased the explained variance to 72%. The total coefficients (fixed + random) revealed clear heterogeneity in the DOC–Rs relationship across soil depths and treatments. Specifically, the total DOC slope was higher in subsoil (8.4) than in topsoil (5.0), whereas the intercept was higher in topsoil (159.1) than in subsoil (149.6), indicating that Rs in subsoil was more sensitive to DOC variation, while topsoil maintained a higher baseline Rs. Across treatments, the total intercept was lowest under LFLT and highest under SFST, whereas the total DOC slope showed the opposite pattern, with higher values under LFLT and LFST and the lowest value under SFST. This suggests that freeze–thaw regimes influenced both the baseline Rs and its responsiveness to DOC. Random-slope deviations further showed that the DOC effect was weaker than the overall average in topsoil but stronger than the overall average in subsoil; similarly, the DOC effect was stronger than average under LFLT and LFST, but weaker than average under SFLT and SFST (Fig. 6). The rANOVA results further showed that inclusion of the DOC random slope at the Depth level significantly improved model fit ($p = 0.035$), whereas the DOC random slope at the Treatment level was not significant (LRT = 3.4, $p = 0.18$). Together, these results indicate that soil depth exerted a stronger regulatory effect than freeze–thaw treatment on the DOC–Rs relationship.

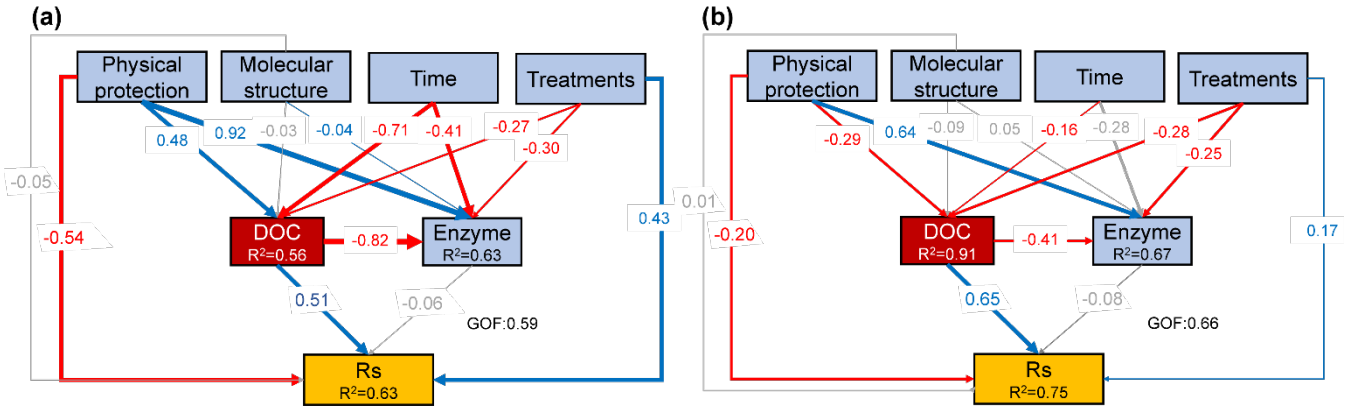

365 **Figure 7: Path analysis results showing the direct and indirect controls of soil organic carbon (SOC) mineralization. Blue and red numbers indicate significant positive and negative relationships ($p < 0.05$), whereas grey numbers indicate non-significant pathways. R^2 is the coefficient of determination, denoting the proportion of variance explained by the model. Panel (a) represents topsoil and panel (b) represents subsoil. Rs denotes the SOC mineralization rate during the thawing phase of each freeze–thaw cycle. Indicators of the latent variables are listed in Table S2, and their loadings are shown in Fig. S8.**

370 When expanding the analysis from the first thawing day to all thawing phases across freeze–thaw cycles, path analysis further clarified these interacting controls (Fig. 7). DOC remained the dominant proximal driver of Rs, with significant positive direct effects in both the topsoil (ρ = 0.51) and subsoil (ρ = 0.65). In contrast, the direct effect of enzyme activity on Rs was weak and non-significant at both depths (ρ = −0.06 and −0.08, respectively). Physical protection also exerted direct negative effects on Rs, but this effect was much stronger in the topsoil (ρ = −0.54) than in the subsoil (ρ = −0.20). Treatments showed
375 significant positive direct effects on Rs (ρ = 0.43 in the topsoil and 0.17 in the subsoil), while simultaneously reducing DOC and enzyme activity, indicating offsetting direct and indirect effects. The time variable, coded to represent incubation progression across the thawing phases, had pronounced negative effects in the topsoil, reducing both DOC (ρ = −0.71) and enzyme activity (ρ = −0.41), whereas its effects were weaker in the subsoil, with a significant negative effect on DOC (ρ = −0.16) and a non-significant effect on enzyme activity (ρ = −0.28). Depth-dependent differences were also evident for physical
380 protection: in the topsoil, it positively affected both DOC (ρ = 0.48) and enzyme activity (ρ = 0.92), whereas in the subsoil it suppressed DOC (ρ = −0.29) but still promoted enzyme activity (ρ = 0.64). Moreover, DOC was negatively associated with enzyme activity in both layers, with a much stronger effect in the topsoil (ρ = −0.82) than in the subsoil (ρ = −0.41), further indicating depth-dependent differences in the coupling between substrate availability and microbial functioning.

4 Discussion

4.1 The importance of FTC frequency

Our results show that SOC mineralization exhibits a sharp and immediate pulse upon thawing (Fig. 1), analogous to the Birch effect observed when dry soils are rewetted (Canarini et al., 2020; Singh et al., 2023). This pulse may represent a rapid reactivation of microbial metabolism and enzyme activity following the release of osmotic and physical constraints during freezing (Chen et al., 2024; Köster et al., 2018; Wang et al., 2010). However, the magnitude of these thaw–induced pulses declined across successive cycles, resulting in progressively lower cumulative mineralization during later thaw phases (Fig. 1). This attenuation likely reflects substrate depletion–given the absence of new carbon inputs in our experimental design – and/or microbial acclimation to repeated stress of freeze (Deng et al., 2024; Li et al., 2023; Lí et al., 2024).

A key finding is that FTC frequency strongly regulates cumulative SOC mineralization (Fig. 2). Soils subjected to many short freeze–thaw oscillations (e.g., the SFLT regime) released substantially more CO_2 than those experiencing fewer, longer cycles (e.g., LFLT), even when the cumulative number of thaw days was identical. Two complementary mechanisms likely explain this pattern. First, each freeze event physically perturbs the soil matrix, disrupting aggregates, weakening organo–mineral associations, and mobilizing DOC and fine particulate material that were previously protected. Multiple short cycles may generate repeated substrate–release events, exposing new pools of labile and intermediate carbon that a single long thaw is less effective at liberating (Liu et al., 2022; Patel et al., 2021). A long thaw may primarily exhaust the most accessible pools, whereas repeated freeze–thaw transitions incrementally unlock additional protected fractions. Second, frequent but short thaws may optimize microbial activation. If microbial reactivation time is short relative to thaw duration, each thaw enables a burst of respiration before substantial resource depletion or physiological stress accumulates. In contrast, a single long thaw may experience declining respiration over time due to substrate exhaustion, transient nutrient imbalances, or shifts in community composition (Li et al., 2023; Lv et al., 2022; Rosinger et al., 2022). Moreover, repeated mild freeze–thaw events typically cause less microbial mortality than a single prolonged or severe freeze, preserving an active decomposer community capable of responding to successive pulses (Isobe et al., 2022; Liu et al., 2020; Pastore et al., 2023). Together, the results demonstrate that FTC frequency is a key and independent driver of SOC turnover, rather than simply a function of thaw duration.

4.2 DOC as the primary and depth–invariant driver

A central finding of this study is that DOC emerged as the most consistent and powerful predictor of SOC mineralization across all freeze–thaw regimes and environmental contexts represented by soil sampling sites and depths. DOC retained its strong influence under every statistical evaluation (zero–order correlations, partial correlations, mixed–effects models, and path analysis) while the effects of enzymatic, structural, and mineralogical variables often diminished or disappeared once DOC was controlled. This convergence underscores the primacy of DOC as the proximal substrate controlling microbial

respiration during freeze–thaw transitions. This should be due to the fact that DOC acts as a comprehensive indicator of substrate accessibility in the context of FTCs, integrating contributions from physicochemical disturbance, microbial turnover, and extracellular enzymatic depolymerization. First, freeze–thaw cycles directly modulate DOC availability by physically altering soil structure. Freezing expands pore water and generates internal pressure that disrupts aggregates and weakens organo–mineral associations, while thawing releases occluded carbon fractions into the dissolved phase (Kim et al., 2023; Wang et al., 2024). This physical perturbation is complemented by biological processes: microbial cells ruptured by freezing liberate cytoplasmic solutes, amino acids, and low–molecular–weight DOC, while membranes and necromass products provide additional labile substrates upon thaw (Deng et al., 2024; Osei et al., 2024). Together, these processes create DOC pulses that microbes can rapidly metabolize, explaining the immediate respiration spikes observed after thaw events (Fig. S3).

The depth–invariant importance of DOC is particularly notable given the stark contrasts in substrate quality, mineral protection, and microbial biomass between topsoils and subsoils (Fig. 3, Fig. S4). Despite these differences, the slope of the DOC–mineralization relationship remained statistically identical across depths. This suggests that once DOC becomes available, microbial communities in depth layers exhibit comparable metabolic responsiveness, regardless of limitations imposed by mineralogy or molecular composition. This finding has two major implications. First, microbial capacity to utilize DOC is ubiquitous throughout the soil profile, even in deep horizons with lower biomass and lower enzyme activities. Second, depth–driven differences in respiration responses to FTCs arise primarily from factors that regulate DOC release, not from differences in microbial utilization efficiency. In other words, depth determines how much DOC becomes available, but not how effectively it is consumed once present. The partial correlation and path analyses strongly support this interpretation. When DOC was controlled, the explanatory power of enzyme activities, pH, mineral–associated carbon, aggregate protection, and molecular carbon fractions was substantially reduced, particularly in the topsoil. In the subsoil, controlling for DOC essentially eliminated all other predictors, leaving DOC as the only significant driver. This pattern indicates that other variables shape mineralization indirectly by influencing DOC production, stabilization, or mobilization rather than by directly controlling metabolic turnover. Enzymes, for instance, become influential primarily by generating DOC from particulate or polymeric matter (Chen et al., 2025; Li et al., 2024b). Mineral surfaces constrain mineralization chiefly by impeding DOC release, sorbing solutes, or shielding particulate C from depolymerization (Georgiou et al., 2022; Lavallee et al., 2020; Zhou et al., 2024). Even molecular composition mattered only when DOC availability was low, particularly in the DOC–limited subsoil environment. These relationships collectively demonstrate that DOC sits at the nexus of microbial, chemical, and physical controls, functioning as the integrative control point of SOC mineralization under freeze–thaw conditions.

4.3 Depth–dependent regulation

While DOC emerged as the most immediate driver of SOC mineralization at both depths, our results reveal pronounced vertical differences in the secondary controls that regulate how FTCs shape substrate accessibility and microbial response.

These depth-dependent constraints, particularly physical protection, temporal progression during incubation, and their influence on DOC–enzyme coupling, determine the extent to which DOC can be mobilized, transformed, or retained during FTCs, and thus explain why topsoils and subsoils differ in their sensitivity to repeated freeze–thaw events. Topsoils showed strong coupling between DOC availability and enzyme activity, reflecting high microbial biomass, active extracellular enzyme pools, and abundant organic substrates (Chen et al., 2025; Deng et al., 2024). In this layer, enzyme activity was closely linked to DOC dynamics rather than exerting a significant direct effect on mineralization, suggesting that its role was mainly indirect within the path network. This pattern indicates that topsoil microbes are well positioned to respond rapidly to thawing events through tight coupling between DOC availability and enzymatic functioning. Consistent with the broader dataset, enzyme activities were generally higher in subsoil than in topsoil, even though microbial biomass was greater in the topsoil, potentially due to higher microbial metabolic activity and substrate availability in the deeper soil horizons (Fig. 3; Fig. 4). This suggests that even though microbial biomass may be greater in the topsoil, the deeper soil layers may have more active microbial communities per unit biomass, contributing to elevated enzyme activities. (Fierer and Jackson, 2006; Stone et al., 2014; Wallenstein and Weintraub, 2008). Consequently, the dominant secondary constraints in topsoil appear to involve the coupling between DOC availability, physical protection, and temporal progression during incubation, rather than direct enzymatic control alone. In subsoils, FTC effects were more strongly constrained by physicochemical controls on DOC release than by direct enzyme-mediated regulation of mineralization.

In contrast, subsoils exhibited fundamentally different controls. Here, physicochemical constraints, especially physical protection rather than molecular structure per se, appeared to play a stronger role in regulating mineralization. Partial correlations revealed that controlling for mineralogical or structural properties eliminated nearly all remaining associations except DOC, indicating that physicochemical constraints dominate subsoil carbon dynamics. These constraints limit the release of DOC during FTCs by stabilizing organic matter on mineral surfaces and within aggregates, reducing both the quantity and quality of substrates accessible during thaw events (Georgiou et al., 2022; Lavallee et al., 2020; Wang et al., 2024). Even though microbial utilization of DOC was efficient once DOC was present, the primary bottleneck in subsoils was substrate liberation, not microbial metabolism. The depth–specific patterns uncovered in the path analysis further reinforce this distinction. In the topsoil, physical protection had strong positive effects on both DOC and enzyme activity, while also exerting a direct negative effect on Rs, suggesting that protected microsites can retain potentially mobilizable substrates and enzymatic potential even when net mineralization remains constrained. In subsoils, however, physical protection influenced mineralization through contrasting pathways, suppressing DOC while enhancing enzyme activity, together with a direct negative effect on Rs. This implies that microbes in deeper horizons rely more heavily on persistent extracellular enzyme pools capable of mobilizing substrates slowly over time, and that FTC–induced structural disturbance is insufficient to overcome the dominant mineralogical constraints governing SOC availability.

These results are broadly consistent with field studies, but field responses are usually more variable. Snow manipulation studies show that changing snow cover (which is closely associated to FTC) can alter soil respiration, DOC, and microbial biomass, but the overall effect depends strongly on site-specific conditions and treatment type. A recent meta-analysis found that snow removal had no significant effect on soil respiration, although it increased DOC, while snow addition increased soil respiration and microbial biomass carbon (Hua et al., 2024; Wipf and Rixen, 2010). In a field study in mid-temperate plantation forests, soil respiration during thawing was 1.54–3.95 times higher than during freezing, and the second freeze–thaw cycle caused a weaker response than the first, which is consistent with the thaw pulses and later attenuation observed in our incubation (Gao et al., 2021b). By contrast, other field observations found that natural variation in snow cover did not change annual soil CO_2 efflux, suggesting that winter responses do not always translate into annual carbon loss (Schindlbacher et al., 2014). Soil translocation studies also show that warming under natural conditions can increase soil CO_2 flux and change labile or particulate carbon pools, but these treatments also alter mean temperature, moisture, and site environment over longer time scales (Li et al., 2024a; Luan et al., 2014). Taken together, our incubation isolates the direct effect of FTC pattern, whereas field snow manipulation and soil translocation studies integrate several processes at the same time.

4.4 Limitations and uncertainties

We highlight several limitations and uncertainties due to the laboratory incubation nature. First, the experimental design is still relatively simple and cannot capture the complexity of FTC dynamics in situ. Particularly, the rate of temperature change in the incubator exceeds that of natural soil temperature changes in natural ambient climatic condition, which may lead to differences in the rate of ice crystal formation and aggregate disruption (Sahoo et al., 2025) and therefore altering substrate protection and accessibility. In addition, related field snow manipulation and soil translocation studies involve simultaneous changes in snow insulation, soil moisture, litter inputs, root activity, and broader site climate, which were intentionally excluded in our laboratory design to isolate the direct effect of FTC regimes. Second, the study did not assess the temporal dynamics of microbial community composition, albeit enzyme activities, CUE and microbial biomass carbon were monitored. The consequence of potential microbial community changes would only manifest over long term (Feng et al., 2007; Ji et al., 2022). Recent studies have suggested that DOC released from freeze–induced cell lysis could preferentially stimulate the proliferation of r–strategist microbes, thereby shifting enzyme production patterns and substrate utilization preferences (Ernakovich et al., 2014; Yuan et al., 2022). In the absence of community composition data, we cannot determine whether the attenuation of CO_2 pulses observed in our experiment was driven by such community–level shifts. However, a plausible interpretation, consistent with earlier work, is that repeated FTCs may gradually select for microbial taxa or physiological traits that are better adapted to recurring stress, thereby reducing the magnitude of respiration pulses over time. This potential mechanism requires direct microbial community profiling to be rigorously tested. For this reason, third, the 48–day incubation may be insufficient to extrapolate findings to directional FTC shifts in long–term. The response of stable SOC pools, such as mineral–associated organic carbon, typically requires months to years of microbial–mineral interactions (Haei et al., 2011;

Turetsky et al., 2020). In addition, repeated FTCs could induce functional adaptation or even evolutionary responses in microbial communities (e.g., upregulation of freeze–tolerance genes), which cannot be captured at the time scale of laboratory manipulation (Leyrer et al., 2024; Razavi et al., 2017)

5 Conclusions

Our results reveal that freeze–thaw cycles regulate SOC mineralization through a hierarchy of controls dominated by DOC availability and modulated by depth–dependent microbial, chemical, and mineralogical constraints. Across all treatments and soil layers, DOC emerged as the most immediate driver of mineralization at both depths, acting as the proximal substrate pool that links physical disturbance, microbial activation, and enzymatic processing during thaw events. This central role of DOC explains the strong respiration pulses observed upon thawing and suggests that FTC frequency can be a stronger determinant of cumulative CO_2 release than thaw duration alone. Repeated freeze–thaw transitions mobilize DOC through structural disruption and microbial turnover, while soils experiencing fewer, longer cycles lack these repeated substrate–release events. At the same time, the capacity of FTCs to generate DOC and sustain mineralization is shaped by vertical heterogeneity in soil properties. In topsoils, stronger biological responsiveness, reflected in tighter DOC–enzyme coupling and greater microbial capacity, likely facilitates rapid conversion of organic substrates into DOC during thawing events. (Gao et al., 2021a; King et al., 2021; Lí et al., 2024), amplifying the effects of frequent FTCs. In subsoils, by contrast, physical protection, together with molecular characteristics of SOC, appears to constrain DOC release, limiting DOC release and reducing sensitivity to FTC frequency. This vertical transition from biologically mediated to chemically and physically constrained SOC turnover underscores the importance of depth–explicit perspectives when evaluating cold–season carbon dynamics.

The findings highlight the need for depth–explicit, mechanistic representations of FTCs in predicting their effects on soil carbon dynamics. First, FTCs should be treated as substrate–mobilizing events, not merely thermal perturbations. Second, vertical heterogeneity across the soil profile must be properly captured: increasing FTC frequency is likely to accelerate topsoil carbon losses, while subsoils may remain buffered unless freeze penetration deepens with changing snow cover or warming–induced variability. Finally, under climate scenarios in which winter warming shortens frozen periods but increases freeze–thaw variability, greater FTC frequency may enhance cold–season carbon losses, with implications for high–latitude and mid–latitude carbon budgets.

Data availability

The data is available from the corresponding author upon reasonable request.

Author contributions

Z.L. conceived and designed the study; S.Z. conducted the field sampling; J.Y. and J.Z. were primarily responsible for the laboratory measurements and incubation experiments, with additional contributions from T.S. and J.M.; J.Y. assessed the data; Z.L. led the writing of the manuscript and interpretation of the results with contributions from J.Y.; M.W. and all authors contributed to discussions and manuscript revision.

Competing interests

The contact author has declared that none of the authors has any competing interests.

Acknowledgements

This research was financially supported by the National Natural Science Foundation of China (grant no. 32241036).

References

Kalbitz, K. and Kaiser, K.: Contribution of dissolved organic matter to carbon storage in forest mineral soils, J. Plant Nutr. Soil Sci., 171, 52–60, https://doi.org/10.1002/jpln.200700043, 2008.

Campbell, J. L., Reinmann, A. B., and Templer, P. H.: Soil freezing effects on sources of nitrogen and carbon leached during snowmelt, Soil Sci. Soc. Am. J., 78, 297–308, https://doi.org/10.2136/sssaj2013.06.0218, 2014.

Canarini, A., Wanek, W., Watzka, M., Sandén, T., Spiegel, H., Šantrůček, J., and Schnecker, J.: Quantifying microbial growth and carbon use efficiency in dry soil environments via ^{18}O water vapor equilibration, Glob. Change Biol., 26, 5333–5341, https://doi.org/10.1111/gcb.15168, 2020.

Chen, X., Cao, J., Sinsabaugh, R. L., Moorhead, D. L., Bardgett, R. D., Fanin, N., Nottingham, A. T., Zheng, X., and Chen, J.: Soil extracellular enzymes as drivers of soil carbon storage under nitrogen addition, Biol. Rev., 100, 1716–1733, https://doi.org/10.1111/brv.70021, 2025.

Chen, Y., Han, M., Qin, W., Hou, Y., Zhang, Z., and Zhu, B.: Effects of whole-soil warming on CH_4 and N_2O fluxes in an alpine grassland, Glob. Change Biol., 30, e17033, https://doi.org/10.1111/gcb.17033, 2024.

Deng, Y., Li, X., Shi, F., and Zhang, Y.: Divergent controlling factors of freeze–thaw-induced changes in dissolved organic carbon and microbial biomass carbon between topsoil and subsoil of cold alpine grasslands, CATENA, 241, 108063, https://doi.org/10.1016/j.catena.2024.108063, 2024.

Dormann, C. F., Elith, J., Bacher, S., Buchmann, C., Carl, G., Carré, G., García Marquéz, J. R., Gruber, B., Lafourcade, B., Leitão, P. J., Münkemüller, T., McClean, C. J., Osborne, P. E., Reineking, B., Schröder, B., Skidmore, A. K., Zurell, D., and

Lautenbach, S.: Collinearity: a review of methods to deal with it and a simulation study evaluating their performance, Ecography, 36, 27–46, https://doi.org/10.1111/j.1600-0587.2012.07348.x, 2013.

Ernakovich, J. G., Hopping, K. A., Berdanier, A. B., Simpson, R. T., Kachergis, E. J., Steltzer, H., and Wallenstein, M. D.: Predicted responses of arctic and alpine ecosystems to altered seasonality under climate change, Glob. Change Biol., 20, 3256–3269, https://doi.org/10.1111/gcb.12568, 2014.

Feng, X., Nielsen, L. L., and Simpson, M. J.: Responses of soil organic matter and microorganisms to freeze–thaw cycles, Soil Biol. Biochem., 39, 2027–2037, https://doi.org/10.1016/j.soilbio.2007.03.003, 2007.

Fierer, N. and Jackson, R. B.: The diversity and biogeography of soil bacterial communities, Proc. Natl. Acad. Sci., 103, 626–631, https://doi.org/10.1073/pnas.0507535103, 2006.

Fierer, N., Colman, B. P., Schimel, J. P., and Jackson, R. B.: Predicting the temperature dependence of microbial respiration in soil: a continental-scale analysis, Glob. Biogeochem. Cycles, 20, https://doi.org/10.1029/2005GB002644, 2006.

Foster, A., Jones, D. L., Cooper, E. J., and Roberts, P.: Freeze–thaw cycles have minimal effect on the mineralisation of low molecular weight, dissolved organic carbon in arctic soils, Polar Biol., 39, 2387–2401, https://doi.org/10.1007/s00300-016-1914-1, 2016.

Gao, D., Liu, Z., and Bai, E.: Effects of in situ freeze-thaw cycles on winter soil respiration in mid-temperate plantation forests, Sci. Total Environ., 793, 148567, https://doi.org/10.1016/j.scitotenv.2021.148567, 2021b.

Gao, Y., Zeng, X., Xie, Q., and Ma, X.: Release of carbon and nitrogen from alpine soils during thawing periods in the eastern Qinghai-Tibet Plateau, Water Air Soil Pollut., 226, 209, https://doi.org/10.1007/s11270-015-2479-2, 2015.

Georgiou, K., Jackson, R. B., Vindušková, O., Abramoff, R. Z., Ahlström, A., Feng, W., Harden, J. W., Pellegrini, A. F. A., Polley, H. W., Soong, J. L., Riley, W. J., and Torn, M. S.: Global stocks and capacity of mineral-associated soil organic carbon, Nat. Commun., 13, 3797, https://doi.org/10.1038/s41467-022-31540-9, 2022.

Haei, M., Rousk, J., Ilstedt, U., Öquist, M. G., Bååth, E., and Laudon, H.: Effects of soil frost on growth, composition and respiration of the soil microbial decomposer community, Soil Biol. Biochem., 43, 2069–2077, https://doi.org/10.1016/j.soilbio.2011.06.005, 2011.

Hair, J. F., Hult, G. T. M., Ringle, C. M., and Sarstedt, M.: A primer on partial least squares structural equation modeling (PLS-SEM), Second edition., SAGE, Los Angeles London New Delhi Singapore Washington DC Melbourne, 363 pp., 2017.

Hua, J., Sun, Q., and Marschner, P.: Immediate and prolonged effects of snow coverage alteration on soil carbon dynamics and microbial activity: A *meta*-analysis, Geoderma, 449, 117029, https://doi.org/10.1016/j.geoderma.2024.117029, 2024.

Isobe, K., Oka, H., Watanabe, T., Tateno, R., Senoo, K., and Shibata, H.: Soil microbial community response to winter climate change is phylogenetically conserved and highly resilient in a cool-temperate forest, Soil Biol. Biochem., 165, 108499, https://doi.org/10.1016/j.soilbio.2021.108499, 2022.

Ji, X., Liu, M., Yang, J., and Feng, F.: Meta-analysis of the impact of freeze–thaw cycles on soil microbial diversity and C and N dynamics, Soil Biol. Biochem., 168, 108608, https://doi.org/10.1016/j.soilbio.2022.108608, 2022.

595 Jobbágy, E. G. and Jackson, R. B.: The vertical distribution of soil organic carbon and its relation to climate and vegetation, Ecol. Appl., 10, 423–436, https://doi.org/10.1890/1051-0761(2000)010%255B0423:TVDOSO%255D2.0.CO;2, 2000.

Joergensen, R. G. and Mueller, T.: The fumigation-extraction method to estimate soil microbial biomass: Calibration of the *k*EN value, Soil Biol. Biochem., 28, 33–37, https://doi.org/10.1016/0038-0717(95)00101-8, 1996.

Kim, Y. J., Kim, J., and Jung, J. Y.: Responses of dissolved organic carbon to freeze–thaw cycles associated with the changes 600 in microbial activity and soil structure, The Cryosphere, 17, 3101–3114, https://doi.org/10.5194/tc-17-3101-2023, 2023.

King, A. E., Rezanezhad, F., and Wagner-Riddle, C.: Evidence for microbial rather than aggregate origin of substrates fueling freeze-thaw induced N2O emissions, Soil Biol. Biochem., 160, 108352, https://doi.org/10.1016/j.soilbio.2021.108352, 2021.

Köster, E., Köster, K., Berninger, F., Prokushkin, A., Aaltonen, H., Zhou, X., and Pumpanen, J.: Changes in fluxes of carbon dioxide and methane caused by fire in Siberian boreal forest with continuous permafrost, J. Environ. Manage., 228, 405–415, 605 https://doi.org/10.1016/j.jenvman.2018.09.051, 2018.

Koven, C. D., Knox, R. G., Fisher, R. A., Chambers, J. Q., Christoffersen, B. O., Davies, S. J., Detto, M., Dietze, M. C., Faybishenko, B., Holm, J., Huang, M., Kovenock, M., Kueppers, L. M., Lemieux, G., Massoud, E., McDowell, N. G., Muller-Landau, H. C., Needham, J. F., Norby, R. J., Powell, T., Rogers, A., Serbin, S. P., Shuman, J. K., Swann, A. L. S., Varadharajan, C., Walker, A. P., Wright, S. J., and Xu, C.: Benchmarking and parameter sensitivity of physiological and vegetation dynamics 610 using the functionally assembled terrestrial ecosystem simulator (FATES) at Barro Colorado Island, Panama, Biogeosciences, 17, 3017–3044, https://doi.org/10.5194/bg-17-3017-2020, 2020.

Lavallee, J. M., Soong, J. L., and Cotrufo, M. F.: Conceptualizing soil organic matter into particulate and mineral-associated forms to address global change in the 21st century, Glob. Change Biol., 26, 261–273, https://doi.org/10.1111/gcb.14859, 2020.

Leyrer, V., Poll, C., Wirsching, J., Kandeler, E., and Marhan, S.: Warming persistently stimulates respiration from an arable 615 soil over a decade, regardless of reduced summer precipitation, Soil Biol. Biochem., 194, 109439, https://doi.org/10.1016/j.soilbio.2024.109439, 2024.

Li, J., He, L., Wang, J., Zhao, X., Chen, J., Ren, C., Wang, J., Guo, Y., and Zhao, F.: Responses of particulate and mineral-associated organic carbon to temperature changes and their mineral protection mechanisms: A soil translocation experiment, Sci. Total Environ., 948, 174689, https://doi.org/10.1016/j.scitotenv.2024.174689, 2024a.

620 Li, J., Wu, J., Yu, J., Wang, K., Li, J., Cui, Y., Shangguan, Z., and Deng, L.: Soil enzyme activity and stoichiometry in response to precipitation changes in terrestrial ecosystems, Soil Biol. Biochem., 191, 109321, https://doi.org/10.1016/j.soilbio.2024.109321, 2024b.

Li, J.-T., Xu, H., Hicks, L. C., Brangarí, A. C., and Rousk, J.: Comparing soil microbial responses to drying-rewetting and freezing-thawing events, Soil Biol. Biochem., 178, 108966, https://doi.org/10.1016/j.soilbio.2023.108966, 2023.

625 Lí, J.-T., Hicks, L. C., Brangarí, A. C., Tájmel, D., Cruz-Paredes, C., and Rousk, J.: Subarctic winter warming promotes soil microbial resilience to freeze–thaw cycles and enhances the microbial carbon use efficiency, Glob. Change Biol., 30, e17040, https://doi.org/10.1111/gcb.17040, 2024.

Li, X., Xie, J., Zhang, Q., Lyu, M., Xiong, X., Liu, X., Lin, T., and Yang, Y.: Substrate availability and soil microbes drive temperature sensitivity of soil organic carbon mineralization to warming along an elevation gradient in subtropical Asia, Geoderma, 364, 114198, https://doi.org/10.1016/j.geoderma.2020.114198, 2020.

Liu, H., Rezanezhad, F., Zak, D., Li, X., and Lennartz, B.: Freeze-thaw cycles alter soil hydro-physical properties and dissolved organic carbon release from peat, Front. Environ. Sci., 10, 930052, https://doi.org/10.3389/fenvs.2022.930052, 2022.

Liu, K., Xu, Y., Feng, W., Zhang, X., Yao, S., and Zhang, B.: Modeling the dynamics of protected and primed organic carbon in soil and aggregates under constant soil moisture following litter incorporation, Soil Biol. Biochem., 151, 108039, https://doi.org/10.1016/j.soilbio.2020.108039, 2020.

Liu, Y., He, N., Zhu, J., Xu, L., Yu, G., Niu, S., Sun, X., and Wen, X.: Regional variation in the temperature sensitivity of soil organic matter decomposition in China's forests and grasslands, Glob. Change Biol., 23, 3393–3402, https://doi.org/10.1111/gcb.13613, 2017.

Luan, J., Liu, S., Chang, S. X., Wang, J., Zhu, X., Liu, K., and Wu, J.: Different effects of warming and cooling on the decomposition of soil organic matter in warm–temperate oak forests: A reciprocal translocation experiment, Biogeochemistry, 121, 551–564, https://doi.org/10.1007/s10533-014-0022-y, 2014.

Lv, Z., Gu, Y., Chen, S., Chen, J., and Jia, Y.: Effects of autumn diurnal freeze–thaw cycles on soil bacteria and greenhouse gases in the permafrost regions, Front. Microbiol., 13, 1056953, https://doi.org/10.3389/fmicb.2022.1056953, 2022.

Lyon, C., Saupe, E. E., Smith, C. J., Hill, D. J., Beckerman, A. P., Stringer, L. C., Marchant, R., McKay, J., Burke, A., O'Higgins, P., Dunhill, A. M., Allen, B. J., Riel-Salvatore, J., and Aze, T.: Climate change research and action must look beyond 2100, Glob. Change Biol., 28, 349–361, https://doi.org/10.1111/gcb.15871, 2022.

Marschner, B. and Kalbitz, K.: Controls of bioavailability and biodegradability of dissolved organic matter in soils, Geoderma, 113, 211–235, https://doi.org/10.1016/S0016-7061(02)00362-2, 2003.

Mathers, N. J., Xu, Z., Berners-Price, S. J., Senake Perera, M. C., and Saffigna, P. G.: Hydrofluoric acid pre-treatment for improving ^{13}C CPMAS NMR spectral quality of forest soils in south-east Queensland, Australia, Aust. J. Soil Res., 40, 665–674, https://doi.org/10.1071/SR01073, 2002.

Meisner, A., Snoek, B. L., Nesme, J., Dent, E., Jacquiod, S., Classen, A. T., and Priemé, A.: Soil microbial legacies differ following drying-rewetting and freezing-thawing cycles, ISME J., 15, 1207–1221, https://doi.org/10.1038/s41396-020-00844-3, 2021.

Miura, M., Jones, T. G., Hill, P. W., and Jones, D. L.: Freeze-thaw and dry-wet events reduce microbial extracellular enzyme activity, but not organic matter turnover in an agricultural grassland soil, Appl. Soil Ecol., 144, 196–199, https://doi.org/10.1016/j.apsoil.2019.08.002, 2019.

He, N., Wang, R., Gao, Y., Dai, J., Wang, X., and Yu, G.: Changes in the temperature sensitivity of SOM decomposition with grassland succession: implications for soil C sequestration, Ecol. Evol., 3, 5045–5054, https://doi.org/10.1002/ece3.881, 2013.

Obu, J., Westermann, S., Bartsch, A., Berdnikov, N., Christiansen, H. H., Dashtseren, A., Delaloye, R., Elberling, B., Etzelmüller, B., Kholodov, A., Khomutov, A., Kääb, A., Leibman, M. O., Lewkowicz, A. G., Panda, S. K., Romanovsky, V.,

Way, R. G., Westergaard-Nielsen, A., Wu, T., Yamkhin, J., and Zou, D.: Northern hemisphere permafrost map based on TTOP modelling for 2000–2016 at 1 km^2 scale, Earth-Sci. Rev., 193, 299–316, https://doi.org/10.1016/j.earscirev.2019.04.023, 2019.

Osei, A. K., Rezanezhad, F., and Oelbermann, M.: Impact of freeze-thaw cycles on greenhouse gas emissions in marginally productive agricultural land under different perennial bioenergy crops, J. Environ. Manage., 357, 120739, https://doi.org/10.1016/j.jenvman.2024.120739, 2024.

Pastore, M. A., Classen, A. T., English, M. E., Frey, S. D., Knorr, M. A., Rand, K., and Adair, E. C.: Soil microbial legacies influence freeze–thaw responses of soil, Funct. Ecol., 37, 1055–1066, https://doi.org/10.1111/1365-2435.14273, 2023.

Patel, K. F., Tatariw, C., MacRae, J. D., Ohno, T., Nelson, S. J., and Fernandez, I. J.: Repeated freeze–thaw cycles increase extractable, but not total, carbon and nitrogen in a Maine coniferous soil, Geoderma, 402, 115353, https://doi.org/10.1016/j.geoderma.2021.115353, 2021.

Razavi, B. S., Liu, S., and Kuzyakov, Y.: Hot experience for cold-adapted microorganisms: Temperature sensitivity of soil enzymes, Soil Biol. Biochem., 105, 236–243, https://doi.org/10.1016/j.soilbio.2016.11.026, 2017.

Rosinger, C., Clayton, J., Baron, K., and Bonkowski, M.: Soil freezing-thawing induces immediate shifts in microbial and resource stoichiometry in luvisol soils along a postmining agricultural chronosequence in western germany, Geoderma, 408, 115596, 2022.

Sahoo, M., Bentley, P., Smith, A., Blackbourn, P., Howarth, K., Bau, D., and Thornton, S.: A laboratory-scale physical model for freeze–thaw studies in soil columns under simulated climate change conditions, Environ. Sci. Pollut. Res., 32, 5293–5301, https://doi.org/10.1007/s11356-025-36053-8, 2025.

Schindlbacher, A., Jandl, R., and Schindlbacher, S.: Natural variations in snow cover do not affect the annual soil CO_2 efflux from a mid-elevation temperate forest, Glob. Change Biol., 20, 622–632, https://doi.org/10.1111/gcb.12367, 2014.

Schmidt, M. W. I., Knicker, H., Hatcher, P. G., and Kogel-Knabner, I.: Improvement of ^{13}C and ^{15}N CPMAS NMR spectra of bulk soils, particle size fractions and organic material by treatment with 10% hydrofluoric acid, Eur. J. Soil Sci., 48, 319–328, https://doi.org/10.1111/j.1365-2389.1997.tb00552.x, 1997.

Schuur, E. A. G., McGuire, A. D., Schädel, C., Grosse, G., Harden, J. W., Hayes, D. J., Hugelius, G., Koven, C. D., Kuhry, P., Lawrence, D. M., Natali, S. M., Olefeldt, D., Romanovsky, V. E., Schaefer, K., Turetsky, M. R., Treat, C. C., and Vonk, J. E.: Climate change and the permafrost carbon feedback, Nature, 520, 171–179, https://doi.org/10.1038/nature14338, 2015.

Schwartz, E.: Characterization of growing microorganisms in soil by stable isotope probing with $H_2{}^{18}O$, Appl. Environ. Microbiol., 73, 2541–2546, https://doi.org/10.1128/AEM.02021-06, 2007.

Singh, S., Mayes, M. A., Kivlin, S. N., and Jagadamma, S.: How the birch effect differs in mechanisms and magnitudes due to soil texture, Soil Biol. Biochem., 179, 108973, https://doi.org/10.1016/j.soilbio.2023.108973, 2023.

Six, J., Elliott, E. T., Paustian, K., and Doran, J. W.: Aggregation and soil organic matter accumulation in cultivated and native grassland soils, Soil Sci. Soc. Am. J., 62, 1367–1377, https://doi.org/10.2136/sssaj1998.03615995006200050032x, 1998.

Song, Y., Zou, Y., Wang, G., and Yu, X.: Altered soil carbon and nitrogen cycles due to the freeze-thaw effect: A meta-analysis, Soil Biol. Biochem., 109, 35–49, https://doi.org/10.1016/j.soilbio.2017.01.020, 2017.

Sorensen, P. O., Finzi, A. C., Giasson, M.-A., Reinmann, A. B., Sanders-DeMott, R., and Templer, P. H.: Winter soil freeze-thaw cycles lead to reductions in soil microbial biomass and activity not compensated for by soil warming, Soil Biol. Biochem., 116, 39–47, https://doi.org/10.1016/j.soilbio.2017.09.026, 2018.

Spaccini, R., Piccolo, A., Conte, P., Haberhauer, G., and Gerzabek, M. H.: Increased soil organic carbon sequestration through hydrophobic protection by humic substances, Soil Biol. Biochem., 34, 1839–1851, https://doi.org/10.1016/S0038-0717(02)00197-9, 2002.

Spohn, M., Klaus, K., Wanek, W., and Richter, A.: Microbial carbon use efficiency and biomass turnover times depending on soil depth – implications for carbon cycling, Soil Biol. Biochem., 96, 74–81, https://doi.org/10.1016/j.soilbio.2016.01.016, 2016.

Stone, M. M., DeForest, J. L., and Plante, A. F.: Changes in extracellular enzyme activity and microbial community structure with soil depth at the luquillo critical zone observatory, Soil Biol. Biochem., 75, 237–247, https://doi.org/10.1016/j.soilbio.2014.04.017, 2014.

Sullivan, B. W., Dore, S., Montes-Helu, M. C., Kolb, T. E., and Hart, S. C.: Pulse emissions of carbon dioxide during snowmelt at a high-elevation site in northern Arizona, USA, Arct. Antarct. Alp. Res., 44, 247–254, https://doi.org/10.1657/1938-4246-44.2.247, 2012.

Tian, H., Lu, C., Yang, J., Banger, K., Huntzinger, D. N., Schwalm, C. R., Michalak, A. M., Cook, R., Ciais, P., Hayes, D., Huang, M., Ito, A., Jain, A. K., Lei, H., Mao, J., Pan, S., Post, W. M., Peng, S., Poulter, B., Ren, W., Ricciuto, D., Schaefer, K., Shi, X., Tao, B., Wang, W., Wei, Y., Yang, Q., Zhang, B., and Zeng, N.: Global patterns and controls of soil organic carbon dynamics as simulated by multiple terrestrial biosphere models: Current status and future directions, Glob. Biogeochem. Cycles, 29, 775–792, https://doi.org/10.1002/2014GB005021, 2015.

Turetsky, M. R., Abbott, B. W., Jones, M. C., Anthony, K. W., Olefeldt, D., Schuur, E. A. G., Grosse, G., Kuhry, P., Hugelius, G., Koven, C., Lawrence, D. M., Gibson, C., Sannel, A. B. K., and McGuire, A. D.: Carbon release through abrupt permafrost thaw, Nat. Geosci., 13, 138–143, https://doi.org/10.1038/s41561-019-0526-0, 2020.

Vance, E. D., Brookes, P. C., and Jenkinson, D. S.: An extraction method for measuring soil microbial biomass C, Soil Biol. Biochem., 19, 703–707, https://doi.org/10.1016/0038-0717(87)90052-6, 1987.

Vaz, M. D. R., Edwards, A. C., Shand, C. A., and Cresser, M.: Determination of dissolved organic phosphorus in soil solutions by an improved automated photo-oxidation procedure, Talanta, 39, 1479–1487, https://doi.org/10.1016/0039-9140(92)80129-2, 1992.

Wallenstein, M. D. and Weintraub, M. N.: Emerging tools for measuring and modeling the *in situ* activity of soil extracellular enzymes, Soil Biol. Biochem., 40, 2098–2106, https://doi.org/10.1016/j.soilbio.2008.01.024, 2008.

Wang, F., Gao, S., Zhang, K., Li, H., Bai, L., Huang, Z., and Mi, C.: Effects of nitrogen application on N2O flux from fluvo-aquic soil subject to freezing-thawing process, Agric. Sci. China, 9, 577–582, https://doi.org/10.1016/S1671-2927(09)60131-0, 2010.

Wang, G., Peng, Y., Chen, L., Abbott, B. W., Ciais, P., Kang, L., Liu, Y., Li, Q., Peñuelas, J., Qin, S., Smith, P., Song, Y., Strauss, J., Wang, J., Wei, B., Yu, J., Zhang, D., and Yang, Y.: Enhanced response of soil respiration to experimental warming upon thermokarst formation, Nat. Geosci., 17, 532–538, https://doi.org/10.1038/s41561-024-01440-2, 2024.

Wipf, S. and Rixen, C.: A review of snow manipulation experiments in arctic and alpine tundra ecosystems, Polar Res., 29, 95–109, https://doi.org/10.1111/j.1751-8369.2010.00153.x, 2010.

Xiang, D., Wang, G., Tian, J., and Li, W.: Global patterns and edaphic-climatic controls of soil carbon decomposition kinetics predicted from incubation experiments, Nat. Commun., 14, 2171, https://doi.org/10.1038/s41467-023-37900-3, 2023.

Yang, X., Chu, D., Hu, H., Deng, W., Chen, J., and Guo, S.: Effects of land-use type and salinity on soil carbon mineralization in coastal areas of northern jiangsu province, Sustainability, 16, 3285, https://doi.org/10.3390/su16083285, 2024.

Yano, Y., McDowell, W. H., and Aber, J. D.: Biodegradable dissolved organic carbon in forest soil solution and effects of chronic nitrogen deposition, Soil Biol. Biochem., 32, 1743–1751, https://doi.org/10.1016/S0038-0717(00)00092-4, 2000.

Yuan, M., Na, M., Hicks, L. C., and Rousk, J.: Will a legacy of enhanced resource availability accelerate the soil microbial response to future climate change?, Soil Biol. Biochem., 165, 108492, https://doi.org/10.1016/j.soilbio.2021.108492, 2022.

Zhou, Z., Ren, C., Wang, C., Delgado-Baquerizo, M., Luo, Y., Luo, Z., Du, Z., Zhu, B., Yang, Y., Jiao, S., Zhao, F., Cai, A., Yang, G., and Wei, G.: Global turnover of soil mineral-associated and particulate organic carbon, Nat. Commun., 15, 5329, https://doi.org/10.1038/s41467-024-49743-7, 2024.

Zhu, L., Ives, A. R., Zhang, C., Guo, Y., and Radeloff, V. C.: Climate change causes functionally colder winters for snow cover-dependent organisms, Nat. Clim. Change, 9, 886–893, https://doi.org/10.1038/s41558-019-0588-4, 2019.